1995_19

AN INTEGRATED COMPARTMENTAL MODEL FOR PREDICTION OF INDOOR RADON CONCENTRATIONS

Kaiss K. Al-Ahmady and David E. Hintenlang
Department of Nuclear Engineering Sciences, University of Florida
Gainesville, FL

ABSTRACT

A carefully selected, heavily instrumented, and fully controlled experimental facility dedicated to research was used to investigate the interaction and effects of key parameters related to the indoor radon problem. Mechanistic and empirical models have been developed in which they return pressure differentials in response to indoor radon driving forces inputs. A semi-diurnal natural pumping model of radon-rich soil gas was based on an exponentially damped response of the sub-slab air volume pressure to changes in atmospheric pressure. A wind-induced pressure differentials model was based on the conservation of energy of the wind speed between the main stream and the structure shell corrected to the effect of wind fluctuation and direction. A temperature-induced pressure differential model was based on the linear approximation of the weakly exponentially-dependent pressures between two temperature zones under hydrostatic equilibrium. Mathematical frameworks were developed to incorporate driving force models into an integrated compartmental model allowed predictions of time-integrated and time-dependent indoor radon concentrations. The integrated model predictions are in good agreement with the observed concentrations at the research site.

INTRODUCTION

Sources of radon entry into structures are divided into three categories: sub-structure soil gas, groundwater and structural materials. Sub-structure soil gas is the main source of radon entering structures and the major contributor to elevated indoor radon concentrations. Radon-rich soil gas can be transported and enter into structures through diffusion and convection processes. The molecular diffusion is driven by the radon concentration gradient between the sub-structure area and the interior. The most significant convective component of radon transport into the interior is due to the pressure-driven air flow processes. Mechanisms which generate pressure gradients depend on environmental and indoor operational factors. The environmental factors that induce pressure differences include temperature differences, wind, meteorological conditions, and atmospheric pressure changes. The indoor operational factors can be divided into two parts: human- and nonhuman- induced indoor operational factors. The nonhuman factors result from mechanically induced pressurization or depressurization of the indoor environment by household appliances, as well as heating, ventilation, and air conditioning (HVAC) systems. Other cases can be represented by the human-induced indoor operational factors, which are characterized by effects such as opening windows and doors.

Wind blowing directly toward a side of a structure may cause an increase in pressure at the structure's wall in order to conserve the change in the momentum initiated by the change of the wind velocity from the free stream to almost zero at the wall, neglecting the effect of the ground. However, wind-induced pressure differentials usually fluctuate rapidly and the determination of the fluctuation frequency has been considered an important parameter (Nazaroff et. al. 1988a). Fukuda (1955) had developed a theoretical treatment to obtain the wind-induced pressure frequency when such pressures are much smaller than atmospheric pressure.

Temperature differences between the indoors and the outdoors can cause air volume movements corresponding to the temperature gradient and, consequently, pressure differences. Further, temperature differences across walls separating air masses can cause pressure differences. The pressure differences also vary with the wall height. This phenomenon is known as the stack effect. Nazaroff et. al. (1987) performed experiments by inducing depressurization in two residential structures with basements to simulate the depressurization that can be generated by wind and temperature differences. They concluded that nearby soil pressure field and air movements are influenced by the temperature induced depressurization of the structures. They also reported the possibility that these effects may account for the higher than average indoor radon concentrations observed in these two houses with basements. Furrer et. al. (1991) reported a significant diurnal dependence between radon concentrations and meteorological conditions. They studied the dynamics of Rn transport from the cellar to the living area in an unheated house and found that strong, long term correlations between temperature differences and pressure differences exist between the indoors and outdoors. Experimental verification for this diurnal dependence is however in most cases profoundly affected by uncontrolled pressure changes across the structure shell due to natural and mechanical ventilation caused by the occupants activities and/or the utilization of the HVAC system.

Al-Ahmady and Hintenlang (1994 a&b) have been utilizing an unoccupied full scale research house to characterize the temperature-driven pressure differentials. They utilized theoretical considerations of pressure differences induced between two zones of different temperature and noted a weakly exponential dependence to develop a mathematical treatment based on a linear approximation to the weakly exponentially dependent pressure difference between temperature zones under hydrostatic equilibrium. They demonstrated that the pressure differences induced by temperature differences between the indoors and outdoors are proportional to both the magnitude of the temperature differences and the average temperature between the indoors and outdoors.

The pressure differences driven by atmospheric pressure variations are probably the most influential environmental parameter driving radon entry. Researchers have proposed that the transient atmospheric pressure changes associated with meteorological conditions can contribute to the radon transport terms (Tsang & Narasimhan 1991, Owczarski et. al. 1990). Al-Ahmady (1992) presented the first experimental observations of the semi-diurnal atmospheric tidal barometric pressure variation as a continuous radon driving force, the natural pumping of radon, for slab-on-grade structures that were built on low permeability soil and fill materials. Hintenlang and Al-Ahmady (1992) demonstrated that these naturally-induced pressure differentials could continue to provide major contributions to radon entry when other sources of house depressurization or pressurization, and consequently outdoor air infiltration rates, are small.

In this work previously developed temperature-induced pressure differences, wind-induced pressure differences, barometric pressure variations-induced pressure differences models; as well as, structure ventilation developed by household appliances are modified to output pressure differentials. These models are then integrated into a mathematical framework governed by the indoor radon gas mass conversation law to form an integrated indoor radon concentration model capable of predicting the average indoor radon entry and concentrations in the indoor environment.

COMPARTMENTS DEVELOPMENT

The general scheme of characterizing the wind-induced pressures on radon entry can be connected to the soil permeability, the frequency of the developed pressure, and the magnitude of the developed pressure differential. More effects are expected to be observed when the frequency of the wind-induced pressure wave is long enough to propagate in the soil and large enough to produce a differential pressure across the structure slab and envelope. Starting from the physics of a fluid in motion, in this case air, the fundamental equation for conservation of fluid energy can be utilized to establish a correlation between wind speed and pressure. In this application, wind is assumed to be represented by an incompressible stream of air that has a Reynolds number much grater than one. Such conditions for this case are always satisfied. Neglecting the shear stress between the wind stream and the ground surface, the conservation of energy indicates that the total air energy under steady-state conditions must be constant at any point in the stream, therefore

$$1/2\, \rho\, v^2 + h\, \rho\, g + P = \text{constant} \qquad (1)$$

where P is the air pressure in Pa, h is the height of the point in meters relative to a horizontal reference, ρ is the air density (kg/m³), g is the acceleration constant due to gravity (m/s²), and v is the air speed (m/s). If the above equation is applied for two points, one in the air stream around the structure when the pressure is not affected yet by the existence of the flow obstruction, and the other at the surface of the structure wall, the second term in the left had side of Equation 1 is neglected for heights encountered in single family residential structures and the speed of wind on the surface of the structure wall is zero then,

$$\Delta P = C_w (P_{in} - P_b - 0.5 \rho v^2) \quad (2)$$

where v is the directional velocity of the wind stream, P_{in} is the indoor pressure, and P_b is the barometric pressure. Equation 2 can be used to characterize wind blowing effects of the structure and consequently on radon driving forces. Detailed predications and development of its applications can be found in the work by Al-Ahmady (1995).

Temperature-Induced pressure differentials can be predicted by implementing the concepts of conservation of forces related to pressure under hydrostatic equilibrium. An analytical solution of the differential equation describing the relation among these forces results in the following relation through utilization of applicable boundary conditions (Al-Ahmady and Hintenlang 1994),

$$P = P_o \exp(-mgh/kT) \quad (3)$$

where m is the mass of air (kg), k is the Boltzmann constant (1.38×10^{-23} J/K), T is the absolute temperature (K), and P_o is the barometric pressure at the reference horizontal level. Applying this equation for two pressure conditions P_1 and P_2, which correspond to temperatures T_1 and T_2, respectively, yields

$$P_1 - P_2 = \Delta P = P_o C \,[(T_1 - T_2)/T_1 T_2] \quad (4)$$

where C is a constant of value 0.0477. This equation can be used to characterize the pressure differences induced by indoor and outdoor temperature difference. Derivation and application of this model can be found from (Al-Ahmady 1995, Al-Ahmady and Hintenlang 1994).

The effects of barometric pressure variations on the radon entry driving forces have been previously developed. The model for predicting pressure differentials across the slab in response to the semi-diurnal natural pumping of radon-rich soil gas was based on an exponentially damped response of the sub-slab air volume pressure to changes in atmospheric pressure. Pressure differentials across the slab can be predicted by (Al-Ahmady 1992, Hintenlang and Al-Ahmady 1992b),

$$\Delta P_{sub} = (P_o(t+\Delta t) - P_o(t)) \exp(-\Delta t/T_R) \quad (5)$$

where T_R is the characteristic equilibrium time, the time required for the spatial sub-slab soil location to equalize with the change in barometric pressure.

The effects of natural and forced ventilation on indoor radon concentrations can be generally attributed to the dilution of indoor radon through mixing with the ambient air which has lower radon concentration. Ventilation forced by pressure differentials, typically lager than one pascal, between the indoor and outdoors and sub-slab area can be estimated from the ASTM blower door testing protocols (ASTM 1987) for differential pressure range from 2 to 50 Pa by the following equation,

$$Q = K (\Delta P)^n \quad (6)$$

where Q is the volumetric flow rate into or out of the structure (m³/s), n is the flow exponent and has a value between 0.5 to 1, and K is the flow coefficient for the structure. K and n need to be empirically determined using a best linear fit for the testing result per the particular structure. For the house utilized in this research, these values are 0.0566 and 0.69 for the flow coefficient and flow exponent, respectively.

INTEGRATED MODEL DEVELOPMENT

Previous section has shown the models describing fundamental radon driving forces. A system approach will be utilized to integrate pressure differential compartments into a mathematical framework in which explicit relationship between pressure differentials and both the indoor radon entry rate and the indoor radon removal rate can be established. Integration of the compartments models can then be developed using the mass balance equation governing radon gas in the indoor volume. The mass balance equation consists of two major components: radon entry and radon removal. Each major component may consist of various radon driving forces components. The basic radon removal mechanisms consist of radon removal by ventilation and the radioactive decay. Estimation of the source term of indoor radon concentration can be divided into four contributing components: entry for sub-structure area by convection and diffusion, entry from potable water, entry from ambient air, and entry from building materials.

Application of the mass balance equation for the radon gas in the indoor environment can be performed by using the differential volume, dV, approach. In the differential volume, the time-rate of change (the accumulation rate) must be equal to the difference between radon generation and removal rates, therefore

$$\frac{dC(t)}{dt} = S(r,t) - RE(r,t) \tag{7}$$

where C(t) is the radon activity concentration in the differential volume (Bq/m^3), S(r,t) is the radon source term in (Bq/m^{3}s) which mostly consists of radon entry from the sub-structure area, and RE(r,t) represents the radon activity removal term from dV in (Bq/m^{3}s). If the above equation is applied for the indoor volume, then

$$\int_v \frac{dC}{dt} dv = \int_v -\lambda C(r,t)\, dv + \int_v -Q(t)\, C(r,t)\, dv + \int_v R(r,t)\, dv \tag{8}$$

where Q(t) is the structure ventilation rate (m^3/s), R(r,t) is the total radon entry rate (Bq/s), and λ is the ^{222}Rn decay constant. If the spatial integration is performed over the volume, rearranging yields

$$\frac{dC(t)}{dt} + \left(\frac{Q(t)}{V} + \lambda\right) C(t) = \frac{R(t)}{V} \tag{9}$$

where V is the indoor volume (m^3).

The above equation is a first order linear differential equation with one independent variable (time). Utilizing the integrating factor method, the general solution is,

$$C(t) = \frac{\int e^{\int (\frac{Q(t)}{V} + \lambda) dt} \frac{R(t)}{V} dt + C}{e^{\int (\frac{Q(t)}{V} + \lambda) dt}} \tag{10}$$

In most practical applications, Q(t) and R(t) do not change during the experimental period encountered in their measurements. If the time distributions of Q(t) and R(t) are available, then time dependent solutions to Equation 9 could be obtained by substituting expressions into Equation 10. However, the system approach has been utilized in this application and a common parameter (ΔP) has been used as an input parameter to the ventilation and entry rates. If the latter parameter is constant over the experimental execution period per each experimental configuration, which is the case for most of the testing, the dependency of ventilation and entry rates on the time inside the integration is negligible, and consequently, they can be treated as constants. Therefore, by performing the integration terms, Equation 10 can be written as,

$$C(t) = \left(\frac{R}{V}\right)\left(\frac{Q}{V} + \lambda\right)^{-1} + C\,e^{-\left(\frac{Q}{V} + \lambda\right)t} \tag{11}$$

This equation represents the general solution to the radon concentration in the indoor environment when the radon entry rate and the structure ventilation rate stay constant, or reasonably constant, during the period of the experiment. The particular solution to Equation 11 can be performed by selecting an initial condition of the indoor radon concentration at the beginning of the experiment which is usually determined by the specific experimental run and testing configuration. If an initial condition of C(t)=0 at t=0 is applied to Equation 11, The effect of the

$$C(t) = \frac{R}{Q + \lambda V}\left(1 - e^{-\left(\frac{Q}{V} + \lambda\right)t}\right) \tag{12}$$

exponential term decreases with time. For the stable indoor radon concentration (steady state), i.e., t>>0, the above solution reduces to,

$$C = \frac{R}{Q + \lambda V} \tag{13}$$

Equation 13 relates the average indoor radon concentration with the structure ventilation and radon entry rates. Neglecting the contributions of building materials and potable water, the total radon entry in Equation 13 consists of three components: (1) the convective flow of soil gas into the structure (R_{conv}), (2) the ambient radon entering the structure with infiltration air (R_{amb}), and (3) the diffusive flow of radon from and through the concrete slab (R_{diff}). Therefore, the total radon entry rate can be written as,

$$R = R_{diff} + R_{amb} + R_{conv} \tag{14}$$

and the individual contributions to the total entry rate can be examined independently.

Convective entry of radon from the sub-structure area into the indoors can be quantified by relating the measured differential pressure across the slab to the corresponding measured indoor radon concentrations, and is depended on the effective entry area into the structure. The least squares fit to experimental results, for the structure encountered in this work, produces a correlation between the pressure differences and the average convective radon entry, with a correlation coefficient (R^2) of 0.9 as,

$$R_{conv} = 13.23\ (\Delta P_{slab}) \tag{15}$$

where R_{conv} in Bq/s and ΔP_{slab} in Pa. This convective entry expression may be extrapolated to lower magnitudes of ΔP_{slab} since convective entry is governed by Darcy's Law which remains proportional to the differential pressure to very small magnitudes (Bear 1972).

Determination of the convective entry from ambient air can be performed from the measured structure ventilation rate and the average radon concentration in ambient air. The latter quantity was measured as approximately 0.5 pCi/l outside the research structure yielding,

$$R_{amb} = Q\,C_{amb} = 1.075\ (\Delta P_{in/out})^{0.69} \tag{16}$$

where R_{amb} in Bq/s and C_{amb} is the average measured ambient concentration of radon. The diffusion entry can then be determined from,

$$R_{diff} = C\,(0.0566\,(\Delta P_{in/out})^{0.69} + 2.0974x10^{-6}) - 1.075\,(\Delta P_{in/out})^{0.69} \tag{17}$$

The total radon entry can be constructed by combining each of the contributing components as,

$$R = 13.23\ \Delta P_{slab} + 1.075\ (\Delta P_{in/out})^{0.69} + R_{diff} \tag{18}$$

where R is in Bq/s and ΔP in Pascal. Application of this equation is limited to the pressure regime $|\Delta P_{in/out}| \geq$ 1 Pa because the relationship quantifying air infiltration rate is not demonstrated for small magnitudes of $\Delta P_{in/out}$. For smaller magnitudes of the indoor/outdoor differential pressure, the observed air infiltration rate, Q, becomes smaller than that predicted by Equation 6. It is experimentally very difficult to maintain constant pressures with reasonable accuracy for pressures that are this small using the blower door. However, Tracer gases measurements may be used to provide time-averaged air exchange rates in this small pressure regime.

Since expressions for both radon entry and removal (by ventilation) have been developed in terms of outputs ΔP, utilization of these expressions in Equation 14 can be employed in each pressure range to predict the average indoor radon entry rate as a function of differential pressures. Incorporating pressure differentials developed by temperature when the indoor pressure is lower than the sub-slab air volume pressure and the outdoor pressure result,

$$R = 13.32\ (P_0\ B\ \frac{T_{ss} - T_{in}}{T_{ss}\ T_{in}}) + 1.07\ (P_0\ B\ \frac{T_{in} - T_{out}}{T_{in}\ T_{out}})^{0.69} + R_{diff} \tag{19}$$

where T_{ss} is the sub-slab air volume temperature and T_{in} is the indoor temperature.

Incorporating the wind-induced pressure differences on the total radon entry can be restricted to the second term of the right hand side of Equation 18 where both convective and diffusive entries from the sub-structure area are considered independent of the wind speed. Such conditions exist if the interaction between the outside area and the sub-slab area through the structure wall interface is negligible, and consequently results in the following expression,

$$R = 13.32\ [(P_b(t+\Delta t)-P_b(t))\ \exp(-\Delta t/T_R)]+1.07\ (P_{in} - P_b - 0.5\ \rho\ v^2)^{0.69} + R_{diff} \tag{20}$$

Incorporating the total average radon entry rate into the average indoor radon expression derived in Equation 13 yields the latter quantity as a function of the compartments differential pressure outputs driven by the temperature, wind, and barometric pressure versions resulting in the following expressions,

$$C1 = \frac{13.23[(P_b(t+\Delta t)-P_b(t))\ \exp(-\Delta t/T_R)] + 1.075\ (P_{in} - P_B - 0.5\ \rho\ v^2)^{0.69}_{leeward} + R_{diff}}{0.0566\ (P_{in} - P_b - 0.5\ \rho\ v^2)^{0.69}_{windward/side} + 8.389x10^{-4}} \tag{21}$$

and,

$$C2 = \frac{13.23\ (0.0477\ P_0\ \frac{T_{ss} - T_{in}}{T_{ss}\ T_{in}}) + 1.075\ (0.0477\ P_0\ \frac{T_{out} - T_{in}}{T_{out}\ T_{in}})^{0.69} + R_{diff}}{0.0566\ (0.0477\ P_0\ \frac{T_{in} - T_{out}}{T_{in}\ T_{out}})^{0.69} + 8.389x10^{-4}} \quad (22)$$

The average indoor radon concentration is then equal to C=C1+C2 (Al-Ahmady 1995). predictions of the indoor radon entry rates and indoor radon concentrations, as well as, parametric analysis for each and combined compartments can be performed using the integrated model. Treatments of independent effects for a particular compartment or of specific combination are specified according to the particular configurations of the structure, the sub-slab area, weather patterns, and the surroundings.

Figure 1 shows the experimental and predicted time-averaged indoor radon concentrations as a function of whole house pressure conditions performed at the University of Florida Radon Research House (UFRRH) used as an experimental facility during the development of models in this work. The diffusion entry rate was measured as 19 Bq/s at the UFRRH and used in the predictions of Figure 1. Figure 2 shows the effect of the sub-slab air volume temperature on the total radon entry rate for a weather pattern of indoor temperature equal to the outdoor temperature and less than the sub-slab air volume temperature. Such patterns particularly examine the convective contribution expressed in the first term of the right hand side of Equation 19 since the convective entry from the ambient is zero. Figure 3 illustrates the predictions of the indoor/outdoor temperature difference on the total radon entry for a weather pattern producing indoor temperature that are equal to the sub-slab air volume temperature and less than the outdoor temperature. This pattern examines the effect of the second term of the right hand side of Equation 19. Figure 4 illustrates the predictions of contributions of wind on the convective radon entry rates for all possible interactions with the structure for four wind speeds. Figure 5 illustrates the predictions of temperature difference effects on the time-averaged indoor radon concentration when the outdoor and sub-slab temperatures are 50° C and the indoor temperature ranges from zero to 50° C.

CONCLUSIONS

Major indoor radon concentration driving forces including those contributing to radon entry rate into the structure and radon removal rate from the structure can be independently modeled as compartments using both mechanistic and empirical approaches. These compartments models can be developed to output differential pressure in response to temperature differences between the indoor and outdoors and the indoors and sub-slab area, barometric pressure versions, wind-blowing on the structure, and utilization of pressure inducing household appliances such as the HVAC systems. The compartment modeling provides a tool to facilitate incorporation of radon driving forces into a mathematical framework governing the accumulation rate of indoor radon concentration. The latter can be developed using the mass balance conservation law for the radon gas in the indoor environment. Utilization of such framework provides mathematical formation where pressure differentials acted as the independent component in a description modeling and consequently allowed systematic integration of the dependent pressure differentials outputs produced in response to temperature, wind, barometric pressure, and household appliances induced radon driving forces. The integrated model can provide predictions for the time-averaged indoor radon entry rates and indoor radon concentrations, as well as, allowing parametric analysis to examine each compartment contributions on the total radon entry and concentrations. Thus it provides a significant tool for analyzing environmental and occupational factors effects on and interaction with, as well as, predictions of, the indoor radon entry rates and concentrations. The integrated model predictions for indoor radon entry and removal rates and the average indoor radon concentrations are in very good agreement with the experimental measurements at the UFRRH.

REFERENCES

Al-Ahmady K.K. Measurements and Theoretical Modeling of Radon Driving Forces and Indoor Radon Concentration and The Development of Radon Prevention and Mitigation Technology, Ph.D. Dissertation, University of Florida, Gainesville, Florida; 1995.

Al-Ahmady, K.K., Measurements and Theoretical Modeling of A Naturally Occurring ^{222}Rn Entry Cycle For Structures Built Over Low Permeability Soils, Master of Engineering Thesis, University of Florida, Gainesville, Florida; 1992.

Al-Ahmady, K.K.; Hintenlang, D.E. Characterization of the Temperature Effects on Radon Driving Forces and Radon Entry for Slab-on-Grade Residential Structures, Health Physics, 66: S59; 1994a.

Al-Ahmady, K.K.; Hintenlang, D.E. Assessment of Temperature-Driven Pressure Differences With Regard to Radon Entry and Indoor Radon Concentration, Proceedings of the 1994 International Radon Symposium, Atlantic City, New Jersey, 1994b; III6.1-III6.11.

ASTM (American Society for Testing and Materials). Standard Test Method for Determining Air Leakage Rate by Fan Pressurization, Philadelphia: ASTM; ASTM E779-87; 1987.

Bear, J. Dynamics of Fluids in Porous Media, Dover Publications, New York; pp. 119-129; 1972.

Fukuda, H. Air and Vapor Movement in Soil Due to Wind Gustiness, Soil Sciences, 79: 249; 1955.

Furrer, D.; Crameri, R.; Burkart, W. Dynamics of Rn Transport From the Cellar to The Living Area in an Unheated House, Health Physics, 60: 393; 1991.

Hintenlang, D.E.; Al-Ahmady, K.K., Pressure Differentials For Radon Entry Coupled to Periodic Atmospheric Pressure Variations, Indoor Air, 2: 208; 1992a.

Hintenlang, D.E.; Al-Ahmady, K.K., Effects of Natural Mechanically Induced Pressurization on Indoor Radon Concentration, Health Physics, 62: S-144; 1992b.

Hintenlang, D.E.; Al-Ahmady, K.K., Building Dynamics and HVAC System Effects on Radon Transport in Florida Houses, The 1992 International Symposium on Radon and Radon Reduction Technology, Vol. 1:VI:93-106, EPA-600/R-93-083a, Springfield, VA. NTIS PB93-196194, 1993.

Hintenlang D.E.; Al-Ahmady, K.K., Influence of Ventilation Strategies on Indoor Radon Concentrations Based on a Semi-Empirical Model for Florida-Style Houses, Health Physics, 66: 427, 1994.

Nazaroff, W.W.; Lewis, S.R.; Doyle, S.M.; Moed, B.A.; Nero, A.V. Experiments on Pollutant Transport from Soil into Residential Basements by Pressure-Driven Airflow, Environmental Science and Technology, 21: 459; 1987.

Nazaroff, W.W.; Moed, B.A.; Sextro, R.G. Soil as a Source of Indoor Radon: Generation, Mitigation and Entry, In: Radon and its Decay Products in Indoor Air, Nazaroff, W.W.; Nero, A.V., eds., John Wiley & Sons, New York, 57-112; 1988.

Tsang, Y.W.; Narasimhan, T.N. Effects of Periodic Atmospheric Pressure Variation on Radon Entry into Buildings, Journal of Geophysical Research, 97: 9161; 1991.

Owczarski, P.C.; Holford, D.J.; Freeman, H.D.; Gee, G.W. Effects of Changing Water Content and Atmospheric Pressure on Radon Flux From Surfaces of Five Soil Types, Geophysical Research Letters, 17, 6: 817; 1990.

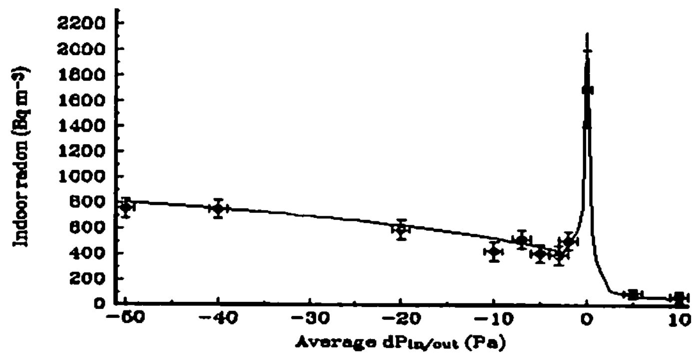

Figure 1: Time-averaged indoor radon concentrations as a function of whole house pressure conditions.

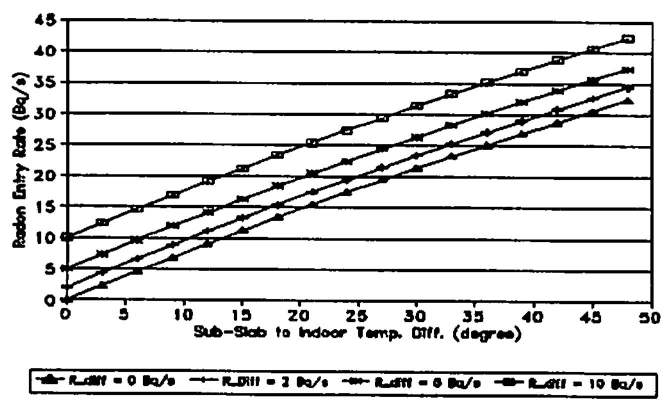

Figure 2: Predicted effects of temperature difference between the sub-slab and the indoors on the total radon entry rate when the indoor temperature is less than the sub-slab area temperature and equal to the outdoor temperature.

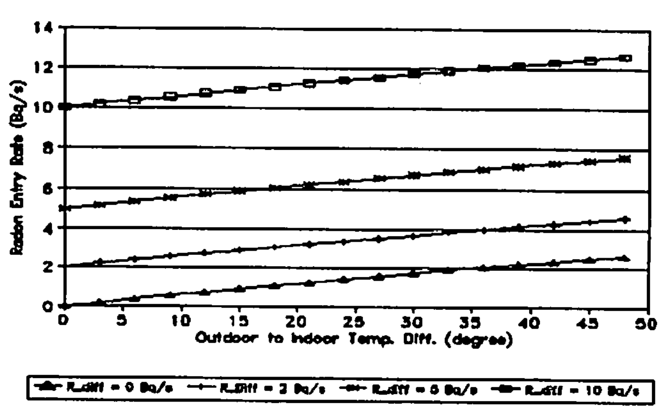

Figure 3: Predicted effect of temperature difference between the indoors and outdoors on the total radon entry rate when the indoor temperature is less than the outdoors and equal to the sub-slab area temperature.

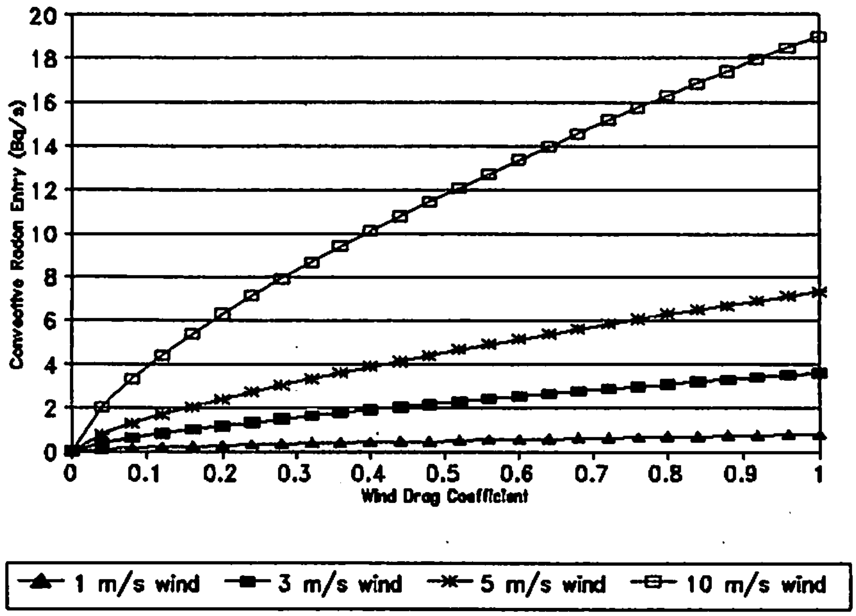

Figure 4: Predictions of the wind speed effects on the convective radon entry rate for the possible range of interaction between the wind and the structure.

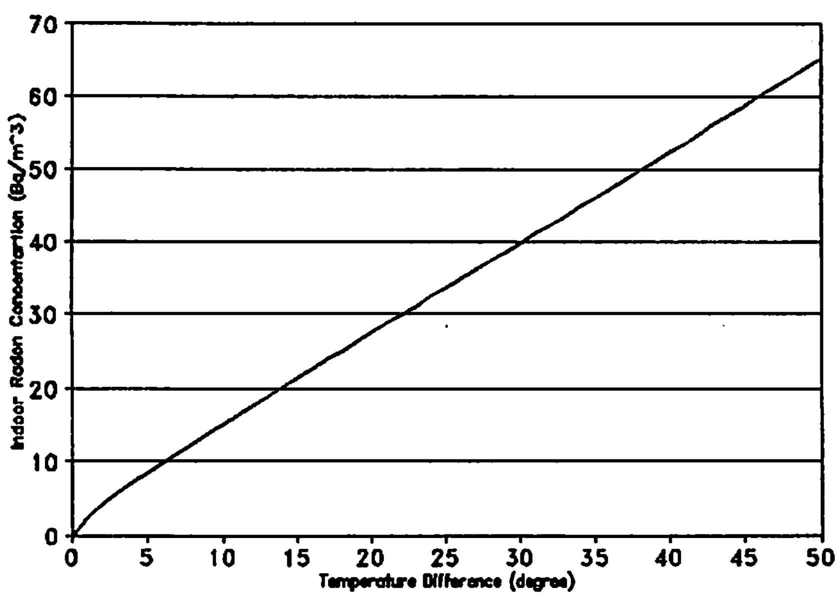

Figure 5: Predictions of the temperature difference effects on the time-averaged indoor radon concentration when the outdoor and sub-slab temperatures are 50° C and the indoor temperature ranges from zero to 50° C.